

Initiation of fatigue cracks in ultrafine-grained copper

P. Lukáš*, L. Kunz, L. Navrátilová

Institute of Physics of Materials, Academy of Sciences of the Czech Republic, Žitkova 22, 616 62 Brno, Czech Republic

Received 11 July 2012, received in revised form 13 August 2012, accepted 20 August 2012

Abstract

Ultrafine-grained copper of commercial purity produced by ECAP technique was tested in fatigue in the range of lives from 5×10^3 to 2×10^{10} cycles. The fatigue strength of ultrafine-grained copper is by a factor of 2 higher than that of conventional-grained copper. The density of surface slip bands decreases with the decreasing stress amplitude and is extremely low in the very-high-cycle region. Fatigue microcracks were found to initiate in cyclic slip bands, which run across many grains in regions of near-by oriented grains. The very first fatigue damage in high-cycle and very-high-cycle regions consists in formation of cavities and elongated voids representing crack nuclei. No grain coarsening was observed either in bulk or in areas underneath the surface slip markings.

Key words: ultrafine-grained microstructure, fatigue, slip bands, microcrack initiation, grain coarsening

1. Introduction

It is now well established that the metals and alloys subjected to severe plastic deformation (SPD) possess ultrafine-grained (UFG) structure and usually exhibit superior yield stress and tensile strength. Recently, the SPD process producing bulk ultrafine-grained UFG structure has started to be termed “nanostructuring” and the resulting material “nanostructured material” [1]. The oldest and most frequently used SPD technique is equal-channel angular-pressing (ECAP) producing materials with an ultra-fine grain size of the order of hundreds of nanometers. UFG materials prepared in this way exhibit in comparison with the conventional grain (CG) size metals and alloys substantially higher tensile strength without substantial loss of their ductility. As for the fatigue strength, nanostructuring has often – but not always – a positive effect. The critical issue in prospective application of nanostructured materials is long-term stability of their UFG structure. It stems from the fact that the structure produced by ECAP (and other SPD techniques as well) is metastable in principle. The severely deformed materials tend to decrease the latent elastic energy by recovery and recrystallization. It inhibits their employment at higher temperatures and it also

leads to the need to carefully examine the long-term stability of UFG structure under fatigue loading. The most intensively studied UFG metal in this respect has been UFG copper. The up to now published results, however, are in some aspects controversial. For example, Agnew et al. [2] and Höppel et al. [3] observed marked heterogeneity of grain structure after plastic strain amplitude controlled fatigue, while Kunz et al. [4] found no grain coarsening after stress controlled fatigue. The reason for the controversy has to be sought in different mode of fatigue control, in different start-up procedure of the fatigue tests, in material purity, technical details of the SPD process, etc.

Fatigue life curves of the UFG metals prepared by ECAP technique have been determined on quite a large scale. The great majority of these data concern low-cycle (LCF) and high-cycle (HCF) fatigue regions, data for very-high-cycle fatigue (VHCF) are practically missing. Besides several hundreds of primary articles also a few overview articles have been written [e.g. 5–7]. Generally it can be stated that the UFG metals exhibit higher fatigue strength than their CG counterparts provided the cycling is stress-controlled. For strain-controlled cycling the effect of nanostructuring is usually inexpressive or even negative. Specifically in the case of copper, the *S-N* curves particularly in

*Corresponding author: tel.: +420 532 290 415; fax: +420 541 212 301; e-mail address: lukas@ipm.cz

Table 1. Chemical composition of UFG copper (wt.%)

Bi	Sb	As	Fe	Ni	Pb	Sn	S	O	Zn	Ag	Cu
0.001	0.002	0.002	0.005	0.002	0.005	0.002	0.004	0.05	0.004	0.003	min. 99.9

the HCF region strongly depend on the purity [e.g. 8] and on the details of the applied ECAP procedure [9]. For decisive majority of the UFG metals it holds that they have a lower resistance against fatigue crack propagation in comparison to CG metals. There are exceptions to this rule. For example, Collini [10] found for UFG copper a higher fatigue crack growth resistance in stage II propagation when compared with CG copper.

To understand the effect of nanostructuring on fatigue process it is important to disclose the mechanisms of fatigue damage in nanostructured materials. This together with the comparison of the mechanisms taking place in UFG material with those taking place in CG material can bring deeper explanation of the effect of nanostructuring on the fatigue strength. Perhaps the most critical damage event in the course of fatigue process is the initiation of the smallest detectable fatigue microcracks having the size of the order of tens to hundreds of nanometers. Investigation of this event in nanostructured copper in HCF and VHCF regions is the main motive for this paper.

2. Experimental

Copper of 99.9 % purity was processed by ECAP technique at the laboratory of Prof. R. Z. Valiev at Ufa State Aviation Technical University (Russia). The limiting content of impurities is given in Table 1. Cylindrical billets 20 mm in diameter and 120 mm in length were produced by route Bc by eight passes with 90° rotation after each extrusion. The deformation was carried out at room temperature. After last ECAP procedure rods of 16 mm in diameter and 100 mm length were turned from the billets.

Tensile properties were determined by means of a standard test on 4 cylindrical specimens of 5 mm in diameter in a Zwick tensile machine. The ultimate tensile strength was found to be 387 ± 5 MPa, the yield stress $\sigma_{0.1} = 349 \pm 4$ MPa, $\sigma_{0.2} = 375 \pm 4$ MPa and the modulus of elasticity $E = 115 \pm 11$ GPa. Grain size determined by transmission electron microscopy was 0.3 microns.

This paper gathers fatigue data obtained on cylindrical specimens under controlled load in symmetrical push-pull cycling ($R = -1$) in three different testing systems:

(i) LCF region: A servo-hydraulic pulser equipped with a clip-on extensometer and data acquisition sys-

tem was used for tests, during which the hysteresis loops were recorded at preset numbers of cycles. The gauge section diameter of the specimens was 6 mm. The frequency of cycling was either 1 Hz or 5 Hz or 10 Hz, while during recording the frequency was decreased to 0.1 Hz. The plastic strain amplitude was taken as the half-width of the hysteresis loop. These tests made it possible to get Coffin-Manson plot.

(ii) HCF region: A resonant fatigue machine operating at frequency of 124 Hz or 213 Hz was used for long-life tests in the range of fatigue lives from about 10^6 to 10^8 ; hysteresis loops were not recorded. The gauge section diameter of the specimens was 6 mm.

(iii) VHCF region: An ultrasonic testing system operating at frequency of 20 kHz was used for the very long-life tests in the range of fatigue lives from 10^8 to 2×10^{10} . For these ultrasonic tests specimens with a minimum diameter 4 mm were used. The specimens were cooled by current of air to keep the temperature of the gauge length below 50°C.

Structural and microstructural investigations were carried out on specimens cycled in HCF and VHCF regions. Gauge length of specimens predestined for surface observation was carefully electrochemically polished. Scanning electron microscope (SEM) Tescan Lyra 3XMU[®] equipped with focused ion beam (FIB) was used for surface and sub-surface observation. Ion channelling technique was applied to reveal the UFG structure.

3. Fatigue life curves

The upper curve in Fig. 1 summarizes the $S-N$ data for all three regions and thus covers the fatigue lives of UFG copper from 5×10^3 to 2×10^{10} cycles. It can be seen that the short life data obtained at low frequencies ranging from 1 to 10 Hz (LCF), the medium life data obtained at frequency 124 Hz or 213 Hz (HCF) and the very long-life data obtained at frequency 20 kHz (VHCF) smoothly concur. This is a strong indication that the frequency effect on the fatigue life is zero or very weak. It is important that all the tests of the UFG copper were carried out on specimens from one batch. There is no analogical set of available $S-N$ data for CG copper obtained on specimens from one batch, cycled under load control and covering the region of fatigue lives from 5×10^3 to 2×10^{10} cycles. For comparison of the UFG with the CG fatigue life curves data taken from our earlier pa-

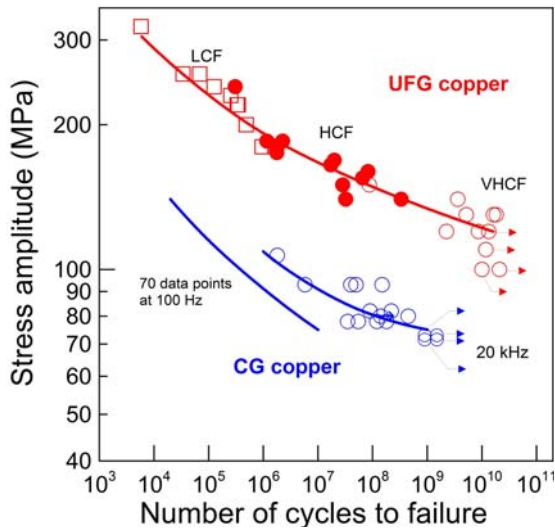


Fig. 1. *S-N* curves of UFG and CG copper specimens.

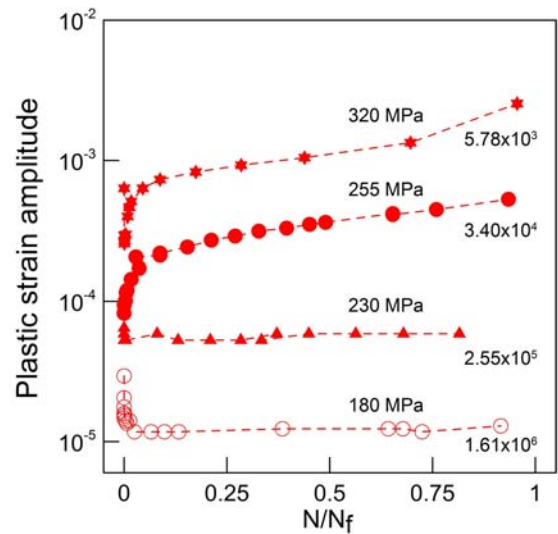


Fig. 3. Hardening/softening curves of UFG copper.

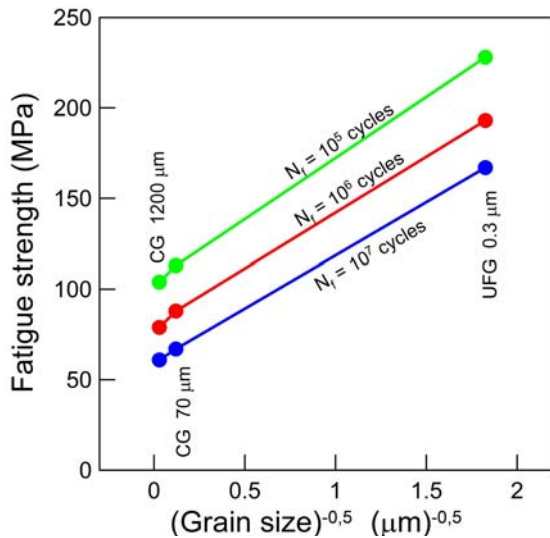


Fig. 2. Fatigue strength of copper in dependence on grain size.

pers [11, 12] are presented in Fig. 1. The two presented sets of life data on CG copper were obtained on specimens from different batches. It is therefore not surprising that the concurrence of the life data of CG copper is not perfect. Nevertheless they were obtained on CG copper (grain size about 70 microns) specimens of purity comparable with the purity of the UFG specimens and also under load controlled cycling. This justifies their employment for comparison. The main outcome of Fig. 1 is that the fatigue strength of UFG copper is by a factor of about 2 higher than that of CG copper in the whole range of fatigue lives including the VHCF region.

The data obtained in HCF region in this paper and

our earlier paper [12] makes it possible to assess the effect of the grain size on the fatigue strength. This is shown in Fig. 2. Here the fatigue strength in terms of the stress amplitudes corresponding to the chosen number of cycles to failure is presented for two CG grain sizes (1200 μm and 70 μm [12]) and one UFG grain size (0.3 μm , this paper). The data are presented in the form of the Hall-Petch relation in which the stress is plotted against the inverse square root of the grain size. The number of data is certainly not sufficient for conclusive statement, but the Fig. 2 indicates that the Hall-Petch relation originally proposed (and many times verified) for the monotonic yield stress could be valid also for the fatigue strength both within the CG region and for comparison of CG and UFG material. How generally is this assertion true and how far it depends also on other factors remains open.

As mentioned above, the LCF fatigue was carried out in such a way that the plastic strain amplitude during the load controlled cycling could be recorded. Figure 3 shows an example of the corresponding hardening/softening curves. The stress amplitudes, σ_a , and the numbers of cycles to failure, N_f , are shown next to the curves. At all the stress amplitudes the plastic strain amplitude drops at the beginning of cycling. This initial hardening is most probably related to the decrease of dislocation density and rearrangement of non-equilibrium structure produced by severe plastic deformation. For higher stress amplitudes the initial hardening is followed by softening. For lower stress amplitudes the effect of cyclic softening vanishes and the initial hardening is followed by the steady state stress-strain response (constant plastic strain amplitude) indicating that the fraction of loaded volume, within which cyclic plasticity can take place, is extremely small. In other words, the fa-

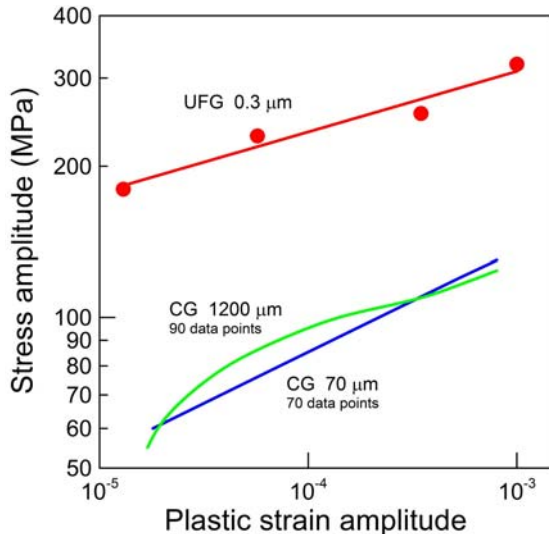


Fig. 4. Cyclic stress-strain curves of UFG and CG copper.

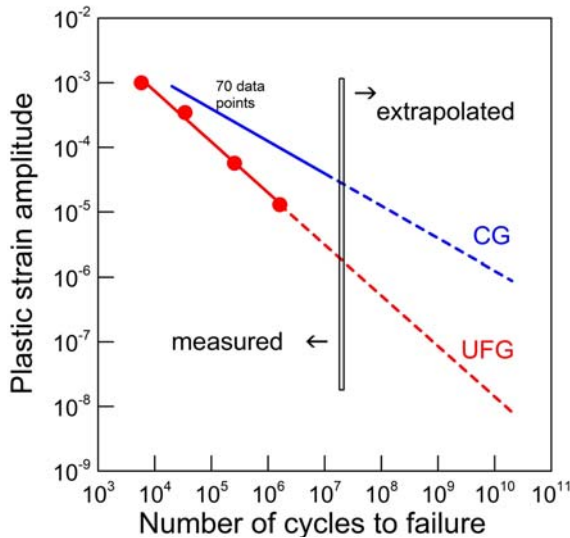


Fig. 5. Measured and extrapolated Coffin-Manson plots for UFG and CG copper.

tigue process at small stress amplitudes is a highly localized phenomenon. The data presented in Figure 3 make it possible to construct cyclic stress-strain curve, i.e. the dependence of the stress amplitude on the plastic strain amplitude at the middle of lifetime ($N/N_f = 0.5$). This curve is shown in Figure 4 together with the cyclic stress-strain curves for CG copper of two substantially different grain sizes taken from our earlier paper [12]. It is clear that the stress amplitude needed to reach plastic strain amplitude 10^{-3} in UFG copper is by a factor of 2 higher than that in CG copper. For the plastic strain amplitude 10^{-5} this factor is even higher, namely about 3.

The cyclic stress-strain curve shown in Fig. 4 can

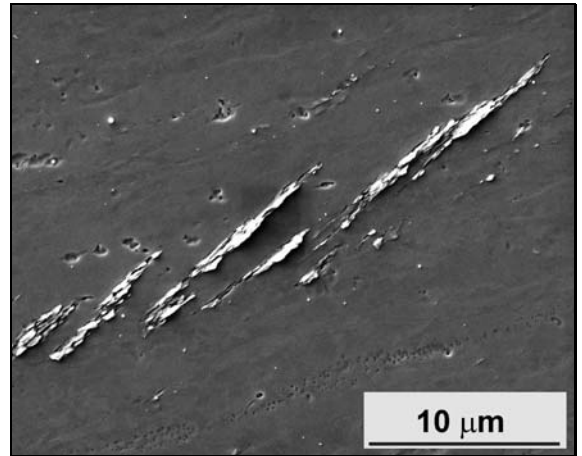


Fig. 6. SEM micrograph of cyclic slip bands in specimen cycled in HCF region.

be used for transformation of the $S-N$ curve into Manson-Coffin curve. This is shown on the left-hand side of Fig. 5; the right-hand side is an extrapolation to the VHCF region. It can be seen that these extrapolated values are very low. Because the direct measurement of the plastic strain amplitude in the ultrasonic cycling by means of strain gauges is possible only for values exceeding 5×10^{-6} and because the indirect methods (thermoelectric and infrared) cannot be used for the determination of the plastic strain amplitudes lower than 10^{-6} [13], the extrapolated data shown in Fig. 5 offer the most probable estimation of the extremely small plastic strain amplitudes in the VHCF region. It can be seen that these values are very low. For the range of lives from 10^8 to 2×10^{10} cycles the corresponding range of plastic strain amplitudes is approximately 8×10^{-9} to 5×10^{-7} . Figure 5 shows also data for CG copper (grain size 70 microns) taken from our earlier paper [12]. It is important that the extrapolated values of the plastic strain amplitudes for CG copper are by about two orders of magnitude higher than those for UFG copper. This point will be discussed later in the section Discussion.

4. Microstructure

An example of surface relief developed on an electrolytically polished specimen after cycling in HCF region ($\sigma_a = 170$ MPa) is shown in Fig. 6. The slip localization is very pronounced. Typically, groups of parallel cyclic slip bands appear on the surface which otherwise does not exhibit any traces of slip activity. The longitudinal lengths of some bands exceed substantially the grain size of the UFG copper (300 nm). Hill (extrusions) and valley (intrusions) topography of the slip bands can be well seen.

Figure 7 presents another example of surface relief,

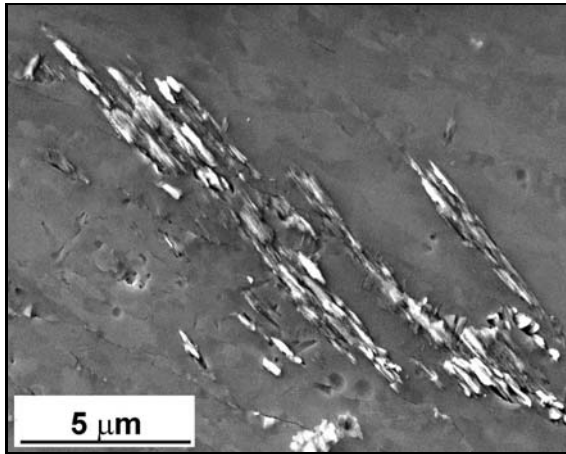


Fig. 7. SEM micrograph of surface slip bands in specimen cycled in VHCF region.

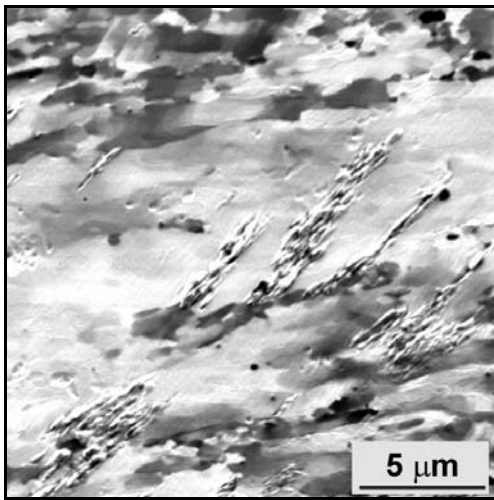


Fig. 8. SEM micrograph of surface slip bands in specimen cycled in VHCF region. Ion-induced secondary electron image.

this time for the case of VHCF cycling. Characteristic feature is the extremely low density of the surface slip bands. More specifically, the surface fatigue slip bands can be seen in the close vicinity of the fatal crack, otherwise their occurrence on the specimen gauge length is extremely rare. Figure 7 presents a SEM micrograph showing one such a rare case. Quite an expressive hill-and-valley topography can be seen. The average length of the slip bands substantially exceeds the grain size of the UFG copper. Figure 8 shows slip bands in VHCF cycled specimen using ion-induced secondary electron image. This type of imaging visualizes both the surface phenomena and the grain orientation. It can be seen that the surface slip bands lie in the zone where the grey contrast of neighbouring grains is low, which indicates that the disorientation

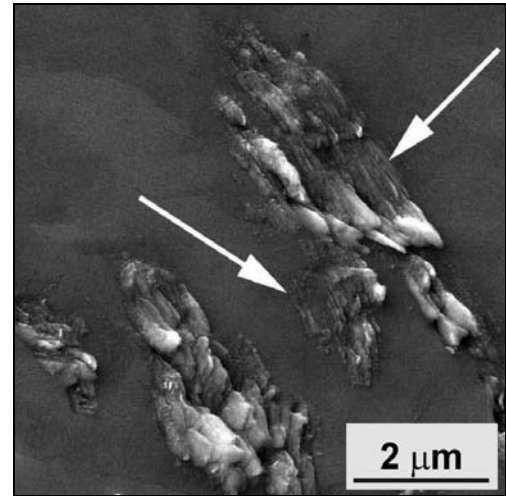


Fig. 9. High magnification SEM micrograph showing slip activity on parallel slip planes within the individual grains (marked by arrows).

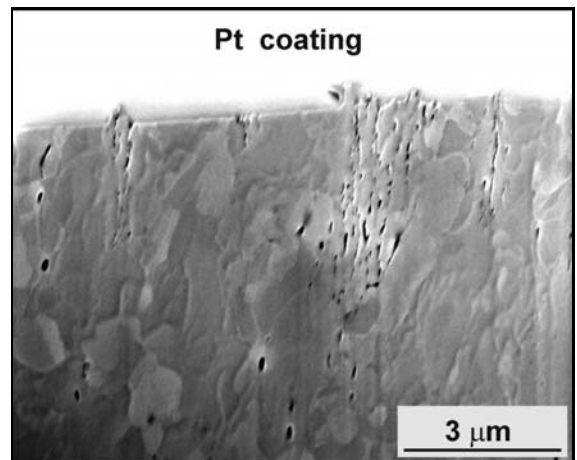


Fig. 10. FIB micrograph showing cut through a set of surface slip bands, underlying grain structure and the embryos of microcracks.

between the grains is small. This zone can be called “zone of near-by oriented grains”. The grains outside this zone have obviously a high mutual disorientation. The size of grains both inside and outside the zone is about 300 nm. The slip bands within the zone of near-by oriented grains develop across many grains. The slip activity within the individual grains can be observed as well. This is documented in Fig. 9 showing clear traces of slip activity on parallel slip planes within the individual grains.

Figure 10 is a FIB micrograph showing an example of a cut perpendicular to surface slip bands. Surface relief and the underlying structure can be seen. No grain coarsening connected with the formation of fatigue slip bands can be stated. The appearance and

size of the grains beneath the surface relief do not differ from those in other places. Numerous crack nuclei can be seen in this FIB micrograph. Some of them are directly connected with the surface roughness. Mechanism of their formation will be discussed later.

5. Discussion

Distribution of the cyclic plastic deformation occurring during fatigue process in the loaded volume of a specimen is not homogeneous. This generally accepted statement seems to be primarily valid for UFG copper. Let us support this assertion by the following extreme example of macroscopic plastic strain amplitude equal to 10^{-8} corresponding to the lifetime of about 1.5×10^{10} cycles (Fig. 5). There are two possibilities how to reach this average value of the plastic strain amplitude: (i) 100 % of the loaded volume deforms cyclically plastically at the plastic strain amplitude of 10^{-8} ; (ii) 0.1 % of the loaded volume deforms cyclically plastically at the plastic strain amplitude of 10^{-5} and 99.9 % of loaded volume deforms only elastically. The value 10^{-5} corresponds to the conventional fatigue limit of UFG copper. Out of the two above possibilities the second possibility is strongly supported by the finding that the fatigue slip markings are very rare in the UFG specimens cycled in VHCF region. Further support comes from the fact that the search for structural changes by means of TEM and EBSD taking place in the bulk of specimens during cycling failed [8]. Thus the significant feature of the UFG copper is highly inhomogeneous distribution of the cyclic plastic strain. In other words, the fatigue process takes place only in a small part of the suitably oriented volume, while the major part of the loaded volume deforms only elastically. The situation in the CG copper is substantially different. Figure 5 shows that for the discussed case of 1.5×10^{10} cycles the extrapolated values of the plastic strain amplitudes for CG copper are by about two orders of magnitude higher than those for UFG copper. Repetition of the above estimation for the value of macroscopic plastic strain amplitude higher by two orders of magnitude, i.e. for 10^{-6} yields that 10 % of the loaded volume deforms cyclically plastically at the plastic strain amplitude of 10^{-5} and 90 % of loaded volume deforms elastically. This is the reason why the cyclic slip activity in the VHCF specimens of CG copper was found to take place in the considerable part of the whole loaded volume [14–17]. For very high plastic strain amplitudes about 10^{-3} and more the two Coffin-Manson curves in Fig. 5 merge; probably whole cycled volumes deform cyclically plastically.

Figure 2 shows that the fatigue strength decreases with the increasing grain size. Whether or not the Hall-Petch representation used in Fig. 2 is justified

remains unanswered, as the number of experimental points is insufficient. Hall-Petch equation is based on the calculation of stress necessary to transfer glide from one grain to its neighbour and is valid for monotonic yield stress for grain sizes varying from 1 mm down to $1 \mu\text{m}$ [18]. Fatigue strength for the given number of cycles to failure is related to the stress amplitude needed for fatigue crack initiation and its propagation. In CG copper the crack initiation occurs in the persistent slip bands. The grain boundaries cause blocking of the persistent slip band spreading. It seems therefore logical that the higher number of grain boundaries (i.e. smaller grain size) leads to higher fatigue strength. The situation in the UFG copper is more difficult. As it can be seen in Fig. 10, the fatigue damage in the form of local discontinuities (cavities) initiate in the slip bands as well, but the slip bands run across many grains and the damage can be seen both in the grains and on the grain boundaries. The viscous glide of the grain boundaries can also contribute to the plastic deformation [18], on the other hand the grain boundaries inhibit slip within the grains. The net result is that the slip band formation and propagation in the interior of the CG grains requires simply lower stress than the slip band formation and propagation across the UFG grain boundaries.

There are papers showing that some UFG metals (including very pure copper) produced by ECAP have a strong tendency to undergo grain coarsening and to develop bimodal grain size structure during cyclic deformation [19]. Fatigue damage in the form of slip bands and microcracks occurs in the region of larger grains. It is important that no grain coarsening at all was observed in our case of UFG copper of commercial purity. Thus the grain coarsening cannot be considered to be a general feature of cycled UFG copper. The FIB micrograph presented in Fig. 10 shows no grain coarsening connected with the surface fatigue slip bands. In other words, the grain coarsening is not a necessary prerequisite for occurrence of fatigue slip bands. Dislocation activity within the boundaries as well as in the inside of the grains leads to slip of nearby oriented grains, to development of surface extrusions and intrusions and to formation of cavities. The rows of cavities below the surface relief seen in Fig. 10 can be considered to be embryos of fatigue cracks. Similar cracks which are considered to be stage I cracks were observed by Weidner et al. [17] in CG copper (grain size 60 microns) subjected to ultrasonic cycling not only in the surface grains, but also in the bulk grains.

6. Conclusions

The main results of the present paper can be summarized as follows.

1. Fatigue microcracks in copper of commercial purity nanostructured by ECAP initiate in cyclic slip bands. Slip bands running across many grains develop in regions of near-by oriented grains. The very first fatigue damage in high-cycle and very-high-cycle regions consists in formation of cavities and elongated voids representing crack nuclei. Their formation is attributed to the dislocation interactions (both within the grain interiors and grain boundaries) producing vacancies which migrate and cluster together in the form of cavities.

2. No grain coarsening was observed. The dynamic grain coarsening, often considered to be related to fatigue damage in nanostructured metals, is not a prerequisite for crack initiation.

3. Fatigue process in ultrafine-grain copper ultrasonically cycled in the very-high cycle fatigue region is a highly localized phenomenon. Estimation based on extrapolation of Coffin-Manson dependence and on the microstructural observations confirms that only an extremely small part of the total loaded volume (of the order of 0.1 %) deforms cyclically plastically, the overwhelming rest deforms cyclically elastically.

4. Fatigue strength of copper decreases with the increasing grain size. This assertion is valid both within the CG region and for comparison of CG and UFG specimens.

Acknowledgement

This work was financially supported by the Czech Science Foundation under contract 108/10/2001. This support is gratefully acknowledged.

References

- [1] Valiev, R. Z., Enikeev, N. A., Langdon, T. G.: *Kovove Mater.*, 49, 2011, p. 1. [doi:10.4149/km.2011.1.9](https://doi.org/10.4149/km.2011.1.9)
- [2] Agnew, S. R., Weertman, J. R.: *Mater. Sci. Eng.*, 244, 1998, p. 145. [doi:10.1016/S0921-5093\(97\)00689-8](https://doi.org/10.1016/S0921-5093(97)00689-8)
- [3] Höppel, H. W., Zhou, Z. M., Mughrabi, H., Valiev, R. Z.: *Phil. Mag. A*, 82, 2002, p. 1781. [doi:10.1080/01418610208235689](https://doi.org/10.1080/01418610208235689)
- [4] Kunz, L., Lukáš, P., Svoboda, M.: *Mater. Sci. Eng.*, 424, 2006, p. 97. [doi:10.1016/j.msea.2006.02.029](https://doi.org/10.1016/j.msea.2006.02.029)
- [5] Vinogradov, A. Y., Hashimoto, S.: *Mater. Trans.*, 42, 2001, p. 74. [doi:10.2320/matertrans.42.74](https://doi.org/10.2320/matertrans.42.74)
- [6] Höppel, H. W., Kautz, M., Xu, C., Murashkin, M., Langdon, T. G., Valiev, R. Z., Mughrabi, H.: *Int. J. Fatigue*, 28, 2006, p. 1001.
- [7] Mughrabi, H., Höppel, H. W.: *Int. J. Fatigue*, 32, 2010, p. 1413. [doi:10.1016/j.ijfatigue.2009.10.007](https://doi.org/10.1016/j.ijfatigue.2009.10.007)
- [8] Lukáš, P., Kunz, L., Svoboda, M.: *Kovove Mater.*, 47, 2009, p. 1.
- [9] Orlov, D., Vinogradov, A.: *Mater. Sci. Eng. A*, 530, 2011, p. 174. [doi:10.1016/j.msea.2011.09.069](https://doi.org/10.1016/j.msea.2011.09.069)
- [10] Collini, L.: *Eng. Fract. Mech.*, 77, 2010, p. 1001. [doi:10.1016/j.engfracmech.2010.02.011](https://doi.org/10.1016/j.engfracmech.2010.02.011)
- [11] Lukáš, P., Kunz, L., Weiss, B., Stickler, R.: *Fatigue Fract. Eng. Mater. Struct.*, 9, 1986, p. 195. [doi:10.1111/j.1460-2695.1986.tb00446.x](https://doi.org/10.1111/j.1460-2695.1986.tb00446.x)
- [12] Lukáš, P., Kunz, L.: *Mat. Sci. Eng.*, 85, 1987, p. 67. [doi:10.1016/0025-5416\(87\)90468-X](https://doi.org/10.1016/0025-5416(87)90468-X)
- [13] Stanzl-Tschegg, B., Schönbauer, B.: *Int. J. Fatigue*, 32, 2010, p. 886. [doi:10.1016/j.ijfatigue.2009.03.016](https://doi.org/10.1016/j.ijfatigue.2009.03.016)
- [14] Mughrabi, H., Stanzl-Tschegg, S.: In: *Proceedings of Fourth International Conference on Very High Cycle Fatigue*. Eds.: Allison, J. E., Jones, J. W., Larsen, J. M., Ritchie, R. O. TMS 2007, p. 75.
- [15] Stanzl-Tschegg, S., Mughrabi, H., Schönbauer, B.: *Int. J. Fatigue*, 29, 2007, p. 2050. [doi:10.1016/j.ijfatigue.2007.03.010](https://doi.org/10.1016/j.ijfatigue.2007.03.010)
- [16] Weidner, A., Amberger, D., Pyczak, F., Schönbauer, B., Stanzl-Tschegg, S., Mughrabi, H.: *Int. J. Fatigue*, 32, 2010, p. 872. [doi:10.1016/j.ijfatigue.2009.04.004](https://doi.org/10.1016/j.ijfatigue.2009.04.004)
- [17] Saada, G.: *Mater. Sci. Eng. A*, 400–401, 2005, p. 146. [doi:10.1016/j.msea.2005.02.091](https://doi.org/10.1016/j.msea.2005.02.091)
- [18] Korn, M., Lapovok, R., Böhner, A., Höppel, H. W., Mughrabi, H.: *Kovove Mater.*, 49, 2011, p. 51. [doi:10.4149/km.2011.1.51](https://doi.org/10.4149/km.2011.1.51)